9-2016

High Speed X-ray Phase Contrast Imaging of Energetic Composites under Dynamic Compression

Niranjan D. Parab
Purdue University

Zane A. Roberts
Purdue University

Michael H. Harr
Purdue University

Jesus O. Mares
Purdue University

Alex D. Casey
Purdue University

See next page for additional authors

Recommended Citation
Parab, N.D., Roberts, Z., Harr, M., Mares, J., Casey, A., Gunduz, I., Hudspeth, M., Claus, B., Sun, T., Fezzaa, K., Son, S. and Chen W., 2016, "High Speed X-ray Phase Contrast Imaging of Energetic Composites under Dynamic Compression," Applied Physics Letters, 109: 131903. https://doi.org/10.1063/1.4963137

Authors
Niranjan D. Parab, Zane A. Roberts, Michael H. Harr, Jesus O. Mares, Alex D. Casey, I. Emre Gunduz, Matthew Hudspeth, Benjamin Claus, Tao Sun, Kamel Fezzaa, Steven F. Son, and Weinong W. Chen

High speed X-ray phase contrast imaging of energetic composites under dynamic compression

Niranjan D. Parab, Zane A. Roberts, Michael H. Harr, Jesus O. Mares, Alex D. Casey, I. Emre Gunduz, Matthew Hudspeth, Benjamin Claus, Tao Sun, Kamel Fezzaa, Steven F. Son, and Weinong W. Chen

Citation: Appl. Phys. Lett. **109**, 131903 (2016);

View online: https://doi.org/10.1063/1.4963137

View Table of Contents: http://aip.scitation.org/toc/apl/109/13

Published by the American Institute of Physics

High speed X-ray phase contrast imaging of energetic composites under dynamic compression

Niranjan D. Parab,[1] Zane A. Roberts,[2] Michael H. Harr,[1] Jesus O. Mares,[1] Alex D. Casey,[2] I. Emre Gunduz,[2] Matthew Hudspeth,[1] Benjamin Claus,[1] Tao Sun,[3] Kamel Fezzaa,[3] Steven F. Son,[1,2] and Weinong W. Chen[1,4]

[1]*School of Aeronautics and Astronautics, Purdue University, West Lafayette, Indiana 47907, USA*
[2]*School of Mechanical Engineering, Purdue University, West Lafayette, Indiana 47907, USA*
[3]*Advanced Photon Source, Argonne National Laboratory, Argonne, Illinois 60439, USA*
[4]*School of Materials Engineering, Purdue University, West Lafayette, Indiana 47907, USA*

(Received 26 July 2016; accepted 8 September 2016; published online 27 September 2016)

Fracture of crystals and frictional heating are associated with the formation of "hot spots" (localized heating) in energetic composites such as polymer bonded explosives (PBXs). Traditional high speed optical imaging methods cannot be used to study the dynamic sub-surface deformation and the fracture behavior of such materials due to their opaque nature. In this study, high speed synchrotron X-ray experiments are conducted to visualize the *in situ* deformation and the fracture mechanisms in PBXs composed of octahydro-1,3,5,7-tetranitro-1,3,5,7-tetrazocine (HMX) crystals and hydroxyl-terminated polybutadiene binder doped with iron (III) oxide. A modified Kolsky bar apparatus was used to apply controlled dynamic compression on the PBX specimens, and a high speed synchrotron X-ray phase contrast imaging (PCI) setup was used to record the *in situ* deformation and failure in the specimens. The experiments show that synchrotron X-ray PCI provides a sufficient contrast between the HMX crystals and the doped binder, even at ultrafast recording rates. Under dynamic compression, most of the cracking in the crystals was observed to be due to the tensile stress generated by the diametral compression applied from the contacts between the crystals. Tensile stress driven cracking was also observed for some of the crystals due to the transverse deformation of the binder and superior bonding between the crystal and the binder. The obtained results are vital to develop improved understanding and to validate the macroscopic and mesoscopic numerical models for energetic composites so that eventually hot spot formation can be predicted. *Published by AIP Publishing.* [http://dx.doi.org/10.1063/1.4963137]

Polymer bonded explosives (PBXs) are composite materials that consist of energetic crystals held together with a polymer binder. Applications include mining, rocket propellants, and main explosive charges in munitions. PBXs may be subjected to various kinds of dynamic loadings during manufacturing, machining, and transport, which may lead to accidental initiation. An improved understanding of non-shock insults to PBXs is needed in order to improve modeling; however, direct optical visualization of these systems is difficult. Consequently, other approaches, such as dynamic X-ray imaging, are of great interest.

The heterogeneous microstructure of a PBX leads to non-uniform stress states, which may cause severe localized material damage and energy dissipation under various types of loadings.[1] Large deformation and damage is associated with the formation of localized energy dissipation or "hot spots."[2] The hot spots formed during mechanical loading may lead to the reaction initiation if they achieve sufficient size and temperature (or energy).[3] Various mechanisms have been proposed for the formation of hot spots in energetic materials, including friction between the sliding and impacting surfaces, localized adiabatic shear of the material during fracture, heating at crack tips, viscous heating of the material during rapid extrusion, and the adiabatic compression of trapped gas spaces.[4,5] Frictional dissipation due to sliding of the crack surfaces generated by both fracture of the crystals and de-bonding is an important mechanism for heat generation.[6,7] The fracture of crystals also leads to the loss of strength of the material, affecting the mechanical integrity, which can further cause viscous heating of the specimen. It is clear that the fracture and de-bonding of the energetic crystals in PBXs are important failure mechanisms that can have significant influence on the initiation under non-shock dynamic loading.

Fracture mechanisms of the energetic crystals (specifically octahydro-1,3,5,7-tetranitro-1,3,5,7-tetrazocine (HMX)) under quasi-static compressive loading have been studied previously.[8] HMX crystals were observed to show an extensive twinning[8] and dislocation slip[9] behavior on the favorable crystal planes prior to fracture. However, the eventual cracking behavior was controlled by the resulting tensile stresses generated by the compressive loading.[8] The behavior of HMX crystals has also been studied under dynamic loading with a particular focus on shock initiation[10,11] and drop weight experiments.[2,12]

The fracture behavior of the PBX specimens has also been studied with uniaxial compression,[13–19] nanoindentation,[20] and Brazilian experiments[21–23] at various strain rates. The de-bonding between the energetic crystals and the binder was the main fracture mode observed in the quasi-static experiments.[14,21,22] As the loading rate was increased, the stiffness of the PBX samples increased[14,15,19] and higher number of crystals were observed to fracture.[14,15,23] The main fracture mechanism for the energetic crystals was the

trans-granular fracture caused by the tensile stress generated due to particle-particle contacts.[15]

The mechanical responses and the fracture behaviors of the PBX depend significantly on the loading rate. However, the deformation and the fracture mechanisms of the PBX materials have not been observed *in situ* under dynamic loading because the sub-surface fracture behavior in energetic crystals cannot be easily captured using the conventional optical high speed imaging methods. Recently, Ramos *et al.* used the high speed X-ray imaging techniques to study the behavior of PBX under high speed impact loading, but the observation of crystal fracture was not reported.[24] The objectives of this study are to investigate the *in situ* deformation and the fracture behavior of PBXs under dynamic compression. A modified Kolsky bar apparatus is used to apply the controlled compressive loading, and a high speed synchrotron X-ray imaging setup is used to record the *in situ* mechanical response of the PBX.

The composite specimens studied here consisted of β-HMX particles embedded in Fe_2O_3 doped hydroxyl-terminated polybutadiene (HTPB). The β-HMX crystals (BAE Systems Grade B, Class 1 (lot BAE13E051–164)) were sieved to obtain a particle size between 425 and 850 μm. The HTPB was fabricated using a mixture of Sartomer R-45HTLO resin and isophorone diisocyanate (IPDI) at an OH index ratio of 1.10 (batches of 10.00 g R-45HTLO: 1.03 g IPDI). Preliminary experiments showed that X-ray imaging contrast was poor; hence, the HTPB was doped with the Firefox 44 μm Fe_2O_3 at 0.25% by mass (0.028 g) to produce a better contrast between the crystals and the binder in the X-ray imaging. The three binder constituents were manually mixed and then degassed in a vacuum chamber for approximately 30 min until there were no visible bubbles. The HTPB-iron oxide mixture was poured into polytetrafluoroethylene (PTFE) molds and the HMX crystals were added, which sank down to a single plane on the bottom of the mold. An additional degassing step was then performed. This mixture was sandwiched between another PTFE plate supported by 1 mm thick shims. The samples were cured at 60 °C in a convection oven for 7 days.[25] After the curing step, the samples were removed from the molds and cut into appropriate shapes for the experiments. The average dimensions of the samples were $2.5 \times 2.5 \times 1.0\,\text{mm}^3$. Each sample contained between 2 and 10 crystals. The weight fraction of the explosives was intentionally kept low so that only one HMX crystal was present in the thickness (X-ray propagation) direction at any given point. Since the X-ray images contain information of the specimen that is integrated over the thickness direction, a single plane of crystals reduced the complexity in analyzing the obtained X-ray images.

The dynamic high strain-rate de-bonding and the fracture behavior of the PBX specimens were investigated using a high speed synchrotron X-ray phase contrast imaging (PCI) synchronized with a modified Kolsky bar apparatus. This setup has been used to study the dynamic fracture mechanisms in various materials, including brittle particles,[26,27] glass plates,[28] high performance fibers,[29] and bone-tissue interfaces.[30] The complete details of the experimental setup

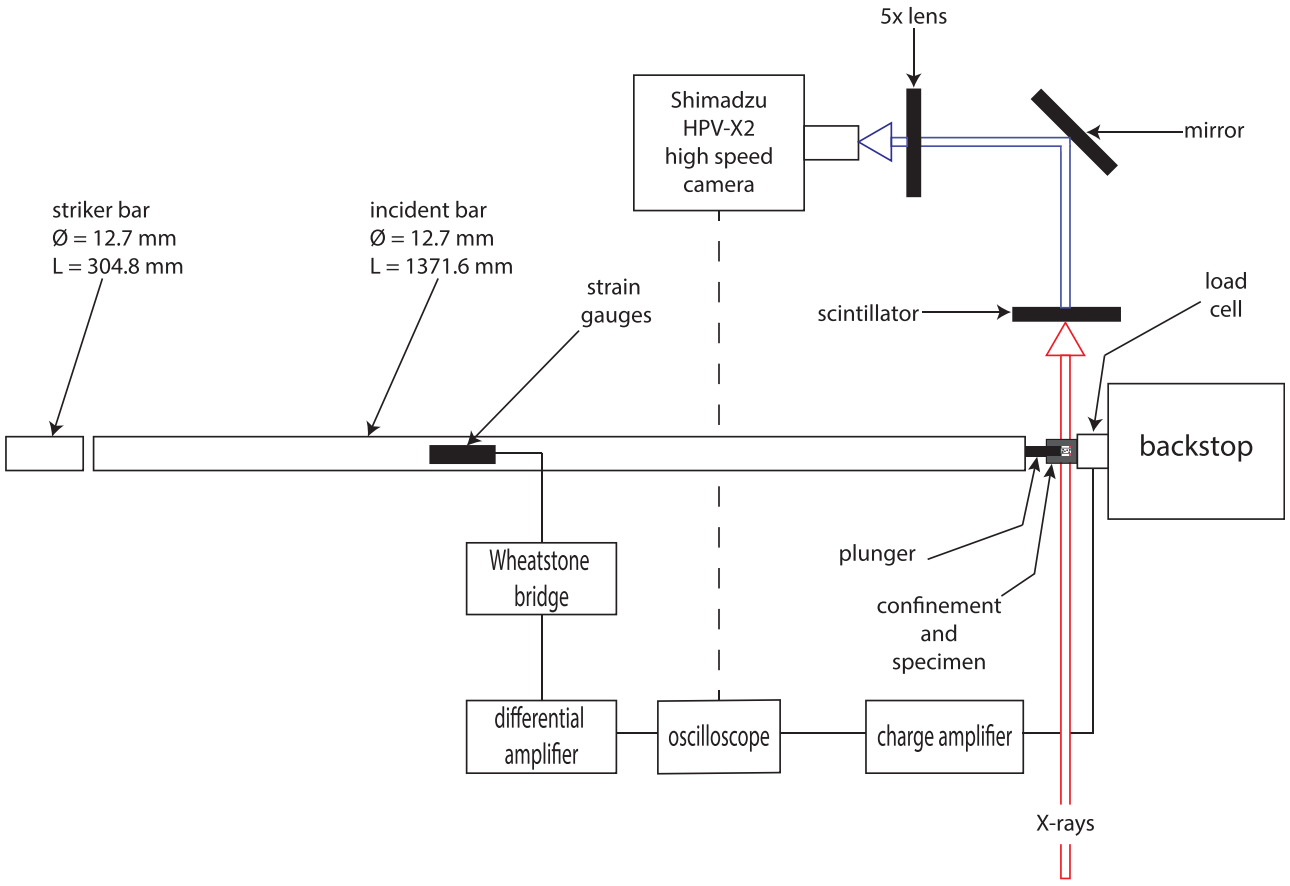

FIG. 1. Schematic of the Kolsky bar apparatus and the X-ray imaging orientation.

are described previously.[30,31] The schematic of the experimental setup is presented in Figure 1.

In a typical synchrotron X-ray source, electron bunches are maintained at relativistic speeds in a circular storage ring and emit X-ray radiation in the direction tangent to the circle. The brilliance of the X-rays is further increased by introducing an undulator into the storage ring.[32] For the experiments reported in this paper, polychromatic, high intensity X-ray PCI measurements were performed at the beam line 32-ID-B, Advanced Photon Source (APS), Argonne National Laboratory. The fundamental energy of the X-rays was centered at 25.0 keV. The size of the X-ray beam on the sample was $2560 \times 1500\ \mu m^2$. The X-ray intensity on the sample was 1.4×10^{16} photons/s/mm^2/0.1% BW. The X-ray PCI exploits the change in the phase of the X-rays as they pass through the sample in order to obtain high contrast images that have higher edge contrast as compared to absorption based X-ray imaging, which is especially beneficial for visualizing cracks and de-bonding in the low absorption materials, such as PBX.[33] The coherence length in the sample plane was 8.6 μm in the horizontal direction and 57.3 μm in the vertical direction. A single crystal $Lu_3Al_5O_{12}$:Ce scintillator (dimensions: 10 mm × 10 mm × 100 μm) was used to convert the propagated X-ray signal to visible light wavelengths. The converted images were relayed to a high speed camera by a 45° mirror, 5× magnification microscope objective, and a tube lens. An ultra-high speed camera (Shimadzu Hyper Vision HPV-X2) was used to record the images at temporal resolutions between 200 ns and 5 μs. For all high speed recordings, the exposure times were between 110 ns and 500 ns, with larger exposure times for the slower recording rates. The resolution of the imaging system was estimated to be 6.4 μm/pixel, and the frame size was 102 000 pixels (400 × 256 pixels).

A Kolsky bar, used to apply the dynamic loading, is commonly used to characterize the material behavior at high strain rates (10^2–10^5 s^{-1}).[34,35] In the current experiment, the Kolsky bar is composed of a striker bar (Ø 12.7 mm, length = 305 mm) and an incident bar (Ø 12.7 mm, length = 1372 mm), both manufactured from a high strength steel alloy (Vascomax 300 maraging steel). In this study, the transmission bar in the conventional Kolsky bar apparatus was replaced with a high impedance load cell (Kistler 9212) mounted on a heavy aluminum backstop. Two semi-conducting strain gauges (Kyowa KSP-2–1K-E4) were attached diametrically to the surface of the incident bar and were connected in a half Wheatstone bridge configuration. The strain gauge assembly was used to record both incident and reflected stress waves. The load cell recorded the force response of the PBX specimens to the incident loading. Both the strain gauge and load signals were collected via an oscilloscope (Tektronix DPO7104C). The recorded load signal was then synchronized with the displacement measurements from the high speed images to obtain force-displacement plots.

For each experiment, a cut specimen was placed in a confinement fixture to restrict motion normal to the surface. Samples were confined between two 1.0 mm thick PMMA plates separated by a 1.0 mm thick steel plate and were centered in a steel channel of 5.0 mm height. The sample holder was then placed between the bar end and the load cell. A photograph of the confinement assembly sandwiched between the bar end and the load cell is presented in Figure 2. A typical experiment started with a manual signal, which triggered the gas gun and launched the striker bar towards one end of the incident bar. The impact of the striker bar with the incident bar generated a compressive stress wave in the bar. As this stress wave propagated along the bar, the resulting strain signal was sensed by the strain gauges and recorded using the oscilloscope. The sensing of the stress wave also provided the trigger for the X-ray shuttering system and the high speed recording system. The stress wave further propagated to the other end of the bar where it pushed the plunger onto the PBX specimen, thus compressing the specimen at a constant velocity of around 6 ms^{-1} (nominal strain rate ≈ 2500 s^{-1}). Appropriate delay times were set for the camera recording to account for the time taken by the wave to propagate from the strain gauge location to the end of the incident bar. The high intensity X-ray beam passed through the PBX specimen as it was being compressed. The deformation and fracture process in the specimen was recorded using the scintillator-camera system. The brightness and the contrast in the recorded high speed images were adjusted using ImageJ software.[36] Further, a colorization scheme was applied (specifically: "look-up table: Fire") to facilitate a better visualization of damage in the specimens.

The high speed X-ray images and the corresponding force-displacement curves from a representative experiment are presented in Figures 3 and 4, respectively. Corresponding slowed down video of the experiment is attached as the integral multimedia material. In the first frame (t = 0 μs), some of the HMX crystals were already in contact with each other. The inherent microstructure and some of the flaws present in the crystals can be observed in the initial state, as expected for standard as-delivered crystals that are used in explosive systems. As the PBX specimen was compressed, the crystals were pressed against each other forming a force chain between the confinement back plate and the plunger. The measured force value was observed to increase at this time. At t = 95 μs, cracking initiated in one of the crystals that was

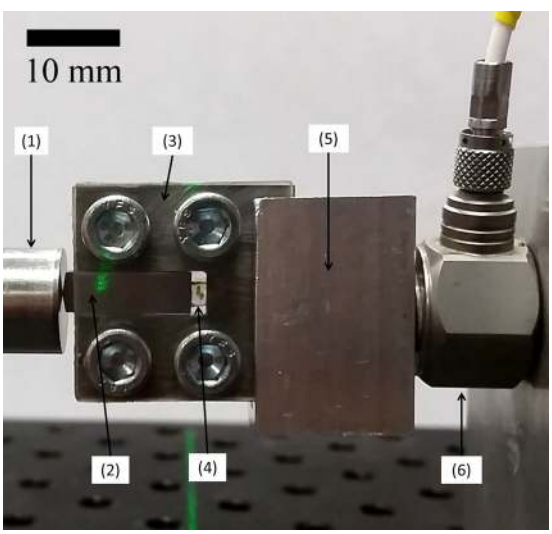

FIG. 2. Image of the specimen confinement fixture sandwiched between the bar-end and the load cell. (1) Bar-end, (2) Plunger, (3) PMMA-steel confinement fixture, (4) HMX-HTPB composite specimen, (5) mounting block attaching the confinement fixture to the load cell, and (6) load cell.

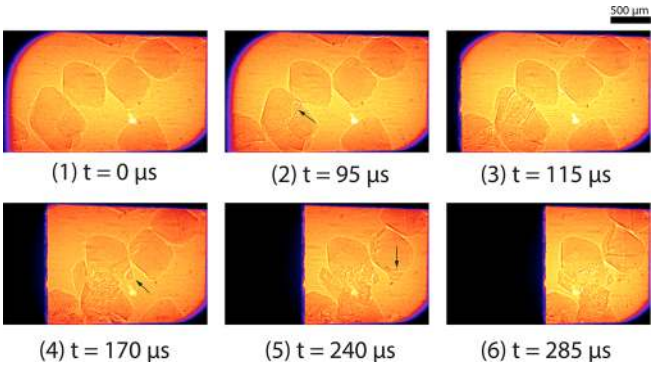

FIG. 3. Image sequence from a representative PBX compression experiment (frame rate = 200 000 fps, exposure time = 500 ns). The arrow in frame (2) shows the initiation of tensile stress driven cracking due to the diametral compressive loading in one of the crystals. Arrows in frames (4) and (5) show the cracking in the crystals due to the tensile stresses generated by the transverse displacement of the binder material. (Multimedia view) [URL: http://dx.doi.org/10.1063/1.4963137.1]

compressed between two other crystals from the contact point. Since the HMX is a brittle material, the critical stress governing fracture in this case is the maximum tensile stress.[8] In a diametral compression case as observed here, the maximum tensile stress occurs normal to the line joining the contact points;[37] hence, the crack developed in the direction that joined the two contact points. As the specimen was compressed further ($t = 115\,\mu s$), the previously cracked crystal was completely fragmented between the contacts. As the crystal was progressively fragmented, the force value remained relatively constant between $t = 95\,\mu s$ and $t = 115\,\mu s$. The crack initiation in the crystal may lead to loss of stiffness in the crystal as well as to the thermal effects due to crack propagation. Both the loss of stiffness and thermal effects may lead to increased initiation and bifurcation of cracks in the pre-cracked crystal. The observation of complete fragmentation of HMX crystals matches the previously reported fracture mechanism for the HMX crystals.[38] On further compression, the tensile stress driven cracking started to initiate in other crystals with cracks developing between the contact points. The area surrounding the first crack was observed to fragment into very small sub-particles upon further compression even in the newly cracked crystals. The measured back face force was observed to decrease after $t = 240\,\mu s$ since transverse displacement of the binder forced one of the crystals to move, thus breaking the force chain. These results show that the crystals retain their ability to carry load even when they are cracked.

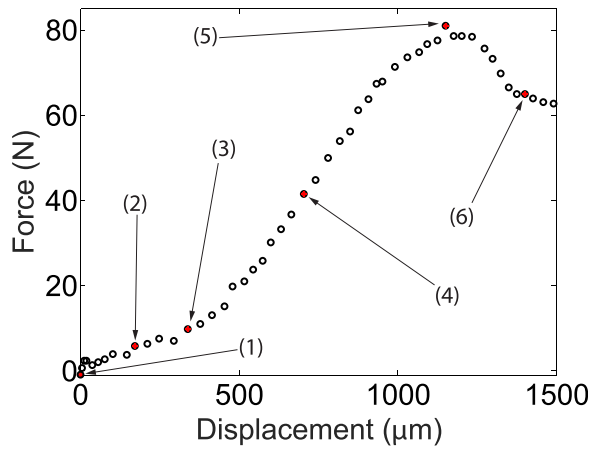

FIG. 4. Corresponding force-displacement curve for the experiment presented in Figure 3. The red markers with associated numbers represent the locations of the frames.

Along with diametral cracking, the crystals were also observed to crack in the locations where large transverse tensile stresses due to the diametral compression of the crystals are not present ($t = 170\,\mu s$ and $240\,\mu s$). It is clear that these cracks were formed due to the tensile stress applied on the crystals by the binder as it moved in the transverse direction. The bonding strength between the binder and the crystal was apparently stronger than the tensile strength of the crystal, and hence, the crystal cracked first before it could de-bond from the binder. These observations are contrary to what was observed previously under quasi-static compression and transverse tensile (Brazilian) loading in which the HMX crystals were observed to de-bond from the estane and rubber binders before they cracked under the transverse tensile stresses.[21,22]

This work confirms mesoscale digital image correlation (DIC) measurements and observations,[39] which describe the deformation mechanisms in polymer bonded sugar simulant as crystal fracture from force chains in the material and the rotation/sliding of crystals. These mechanisms are dependent on the volume fraction of crystals of the specific composite system.

To conclude, a high speed synchrotron X-ray PCI setup was synchronized with a modified Kolsky bar apparatus to observe the deformation and the fracture behavior of the PBX under dynamic compressive loading. The main fracture mode for the HMX crystals was observed to be the tensile stress driven cracking under diametral compression. However, the transverse deformation of the binder also induced the tensile stress on the crystals due to excellent binding between crystals and the binder, which led to cracking in some crystals. These real-time observations of deformation and fracture mechanisms provide more insight into the behavior of PBX under dynamic loading and will be valuable in verifying the mesoscale numerical models of PBXs to improve the understanding of hot spot formation.

The authors acknowledge the technical and safety help from Alex Deriy at beam line 32, APS. Funding for this work was provided by the Air Force Office of Scientific Research Award No. FA9550-15-1-0102 (program managers: Dr. Jennifer Jordan and Dr. Martin Schmidt). This research used resources of the Advanced Photon Source, a U.S. Department of Energy (DOE) Office of Science User Facility operated for the DOE Office of Science by Argonne National Laboratory under Contract No. DE-AC02-06CH11357. J. O. Mares acknowledges the National Science Foundation Graduate Research Fellowship Program under Grant No. DGE-1333468.

[1]A. Barua, Y. Horie, and M. Zhou, "Microstructural level response of HMX–Estane polymer-bonded explosive under effects of transient stress waves," Proc. R. Soc. London, Ser. A **468**(2147), 3725–3744 (2012).
[2]J. E. Field, G. M. Swallowe, and S. N. Heavens, "Ignition mechanisms of explosives during mechanical deformation," Proc. R. Soc. London, Ser. A **382**(1782), 231–244 (1982).

[3]C. M. Tarver, S. K. Chidester, and A. L. Nichols, "Critical conditions for impact- and shock-induced hot spots in solid explosives," J. Phys. Chem. **100**(14), 5794–5799 (1996).
[4]J. E. Field, "Hot spot ignition mechanisms for explosives," Acc. Chem. Res. **25**(11), 489–496 (1992).
[5]J. E. Field, N. K. Bourne, S. J. P. Palmer, S. M. Walley, J. Sharma, and B. C. Beard, "Hot-spot ignition mechanisms for explosives and propellants [and discussion]," Philos. Trans. R. Soc. London, Ser. A **339**(1654), 269–283 (1992).
[6]J. K. Dienes, Q. H. Zuo, and J. D. Kershner, "Impact initiation of explosives and propellants via statistical crack mechanics," J. Mech. Phys. Solids **54**(6), 1237–1275 (2006).
[7]E. M. Hunt, S. Malcolm, and M. Jackson, "High-speed study of drop-weight impact ignition of PBX9501 using infrared thermography," ISRN Mech. Eng. **2011**, 1–4.
[8]S. J. P. Palmer and J. E. Field, "The deformation and fracture of β-HMX," Proc. R. Soc. London, Ser. A **383**(1785), 399–407 (1982).
[9]H. G. Gallagher, J. N. Sherwood, and R. M. Vrcelj, "Growth and dislocation studies of β-HMX," Chem. Cent. J. **8**(1), 1–11 (2014).
[10]J. Dick, "Measurement of the shock initiation sensitivity of low density HMX," Combust. Flame **54**(1–3), 121–129 (1983).
[11]H. K. Springer, K. S. Vandersall, C. M. Tarver, and P. S. Souers, "Investigating shock initiation and detonation in powder HMX with reactive mesoscale simulations," paper presented at 15th International Detonation Symposium, San Francisco, CA, USA, 13–18 Jul 2014.
[12]Y.-Q. Wu, F.-L. Huang, and Z.-Y. Zhang, "Experiments and modeling of HMX granular explosives subjected to drop-weight impact," RSC Adv. **2**(10), 4152–4163 (2012).
[13]D. A. Wiegand and J. J. Pinto, "The composition of polymer composite fracture surfaces as studied by XPS," (MRS Proc., 1995), Vol. 409, p. 281.
[14]G. T. Gray, D. J. Idar, W. R. Blumenthal, C. M. Cady, and P. D. Peterson, "High- and low-strain rate compression properties of several energetic material composites as a function of strain rate and temperature, Los Alamos National Laboratory, NM (United States)," Report No. LA-UR-98-3059, CONF-980803–, 1998.
[15]P. Chen, F. Huang, K. Dai, and Y. Ding, "Detection and characterization of long-pulse low-velocity impact damage in plastic bonded explosives," Int. J. Impact Eng. **31**(5), 497–508 (2005).
[16]Z. Zhou, P. Chen, Z. Duan, and F. Huang, "Study on fracture behaviour of a polymer-bonded explosive simulant subjected to uniaxial compression using digital image correlation method," Strain **48**(4), 326–332 (2012).
[17]C. Park, H. Huh, and J. Park, "Rate-dependent hardening model for polymer-bonded explosives with an HTPB polymer matrix considering a wide range of strain rates," J. Compos. Mater. **49**, 425–438 (2015).
[18]W. R. Blumenthal, "Influence of temperature and strain rate on the mechanical behavior of PBX 9502 and Kel-F 800^{TM}," AIP Conf. Proc. **505**, 671–674 (2000).
[19]Y. C. Xiao, Y. Sun, X. Li, Q. H. Zhang, S. W. Liu, and H. Yang, "Dynamic mechanical behavior of PBX," Propellants, Explos. Pyrotech. **41**, 629–636 (2016).
[20]J. D. Yeager, K. J. Ramos, S. Singh, M. E. Rutherford, J. Majewski, and D. E. Hooks, "Nanoindentation of explosive polymer composites to simulate deformation and failure," Mater. Sci. Technol. **28**(9–10), 1147–1155 (2012).
[21]S. J. P. Palmer, J. E. Field, and J. M. Huntley, "Deformation, strengths and strains to failure of polymer bonded explosives," Proc. R. Soc. London, Ser. A **440**(1909), 399–419 (1993).
[22]P. J. Rae, H. T. Goldrein, S. J. P. Palmer, J. E. Field, and A. L. Lewis, "Quasi–static studies of the deformation and failure of β–HMX based polymer bonded explosives," Proc. R. Soc. London, Ser. A **458**(2019), 743–762 (2002).
[23]L. I. Jun-Ling, F. U. Hua, T. A. N. Duo-Wang, L. U. Fang-Yun, and C. H. E. N. Rong, "Fracture behaviour investigation into a polymer-bonded explosive," Strain **48**(6), 463–473 (2012).
[24]K. J. Ramos, B. J. Jensen, A. J. Iverson, J. D. Yeager, C. A. Carlson, D. S. Montgomery, D. G. Thompson, K. Fezzaa, and D. E. Hooks, "In situ investigation of the dynamic response of energetic materials using IMPULSE at the advanced photon source," J. Phys. Conf. Ser. **500**(14), 142028 (2014).
[25]M. A. Daniel, "Polyurethane binder systems for polymer bonded explosives," Edinburgh, Australia, 2006, Report No. DSTO-GD-0492.
[26]N. D. Parab, B. Claus, M. C. Hudspeth, J. T. Black, A. Mondal, J. Sun, K. Fezza, X. Xiao, S. N. Luo, and W. W. Chen, "Experimental assessment of fracture of individual sand particles at different loading rates," Int. J. Impact Eng. **68**, 8–14 (2014).
[27]M. B. Zbib, N. D. Parab, W. W. Chen, and D. F. Bahr, "New pulverization parameter derived from indentation and dynamic compression of brittle microspheres," Powder Technol. **283**, 57–65 (2015).
[28]N. D. Parab, J. T. Black, B. Claus, M. Hudspeth, J. Sun, K. Fezzaa, and W. W. Chen, "Observation of crack propagation in glass using X-ray phase contrast imaging," Int. J. Appl. Glass Sci. **5**(4), 363–373 (2014).
[29]M. Hudspeth, B. Claus, N. Parab, B. Lim, W. Chen, T. Sun, and K. Fezza, "In situ visual observation of fracture processes in several high-performance fibers," J. Dyn. Behav. Mater. **1**(1), 55–64 (2015).
[30]W. W. Chen, M. C. Hudspeth, B. Claus, N. D. Parab, J. T. Black, K. Fezza, and S. N. Luo, "In situ damage assessment using synchrotron X-rays in materials loaded by a Hopkinson bar," Philos. Trans. R. Soc. London, Ser. A **372**(2015), 20130191 (2014).
[31]M. Hudspeth, B. Claus, S. Dubelman, J. Black, A. Mondal, N. Parab, C. Funnell, F. Hai, M. L. Qi, S. N. Luo, and W. Chen, "High speed synchrotron x-ray phase contrast imaging of dynamic material response to split Hopkinson bar loading," Rev. Sci. Instrum. **84**, 025102 (2013).
[32]A. Balerna and S. Mobilio, "Introduction to synchrotron radiation," in *Synchrotron Radiation Basics Methods and Applications*, 1st ed., edited by S. Mobilio, F. Boscherini, and C. Meneghini (Springer-Verlag, Berlin, 2015), pp. 3–28.
[33]S. W. Wilkins, T. E. Gureyev, D. Gao, A. Pogany, and A. W. Stevenson, "Phase-contrast imaging using polychromatic hard X-rays," Nature **384**, 335 (1996).
[34]H. Kolsky, "An investigation of the mechanical properties of materials at very high rates of loading," Proc. Phys. Soc. London, Ser. B **62**, 676 (1949).
[35]W. W. Chen and B. Song, *Split Hopkinson (Kolsky) Bar: Design, Testing and Applications* (Springer, New York, 2011).
[36]C. A. Schneider, W. S. Rasband, and K. W. Eliceiri, "NIH Image to ImageJ: 25 years of image analysis," Nat. Methods **9**(7), 671–675 (2012).
[37]Y. Hiramatsu and Y. Oka, "Determination of the tensile strength of rock by a compression test of an irregular test piece," Int. J. Rock Mech. Min. Sci. **3**, 89–99 (1966).
[38]P. D. Peterson, M. A. Fletcher, and E. L. Roemer, "Influence of pressing intensity on the microstructure of PBX 9501," Energy Mater. **21**(4), 247–260 (2003).
[39]S. Ravindran, A. Tessema, and A. Kidane, "Local deformation and failure mechanisms of polymer bonded energetic materials subjected to high strain rate loading," J. Dyn. Behav. Mater. **2**, 146–156 (2016).